Astron. Astrophys. 363, 1040–1050 (2000)

ASTRONOMY AND ASTROPHYSICS

Cool helium-rich white dwarfs from the Hamburg/ESO survey⋆,⋆⋆

S. Friedrich[1,2], **D. Koester**[1], **N. Christlieb**[3], **D. Reimers**[3], **and L. Wisotzki**[3]

[1] Universität Kiel, Institut für Theoretische Physik und Astrophysik, 24098 Kiel, Germany
[2] Astrophysikalisches Institut Potsdam, An der Sternwarte 16, 14482 Potsdam, Germany
[3] Universität Hamburg, Hamburger Sternwarte, Gojenbergsweg 112, 21029 Hamburg, Germany

Received 23 May 2000 / Accepted 20 September 2000

Abstract. We present an analysis of 40 cool helium-rich white dwarfs found in the Hamburg/ESO survey. They were selected for follow-up spectroscopy because of their $U-B$ colour below -0.18, the absence of strong absorption lines, and a continuum shape similar to that of a quasar. Effective temperatures for individual stars were determined by fitting model atmospheres of nearly pure helium with a small admixture of hydrogen. As a consequence of the selection criteria all but one sample stars have $T_{\rm eff}$ below 20000 K. Four stars clearly show helium and hydrogen lines in their spectra. In the spectra of another three, helium, hydrogen, and metal lines can be detected. For these stars hydrogen and metal abundances were also determined by fitting appropriate model atmospheres containing these elements. Seven sample stars most likely have helium-rich atmospheres but do not show any helium lines. They either have featureless spectra or show calcium lines.

Key words: surveys – stars: fundamental parameters – stars: white dwarfs

1. Introduction

The Hamburg/ESO Survey for bright quasars (HES, Wisotzki et al. 1996) was initiated in 1990 to perform a spectroscopic survey, based on digitized objective-prism photographs taken with the ESO Schmidt telescope, in the southern hemisphere. A nominal area of $9500\,\mathrm{deg}^2$ in the southern sky is covered with an average limiting magnitude on the prism plates of $B\sim 17.5$. It was conceived as a complement to the Hamburg Quasar Survey (HQS, Hagen et al. 1995), which aims at a complete coverage of the northern sky except for the galactic plane. Similar surveys have been conducted in the past to search for faint blue objects. Still in progress in the southern hemisphere are the Edinburgh-Cape survey (Stobie et al. 1997), the Homogeneous Bright Quasar Survey (Cristiani et al. 1995), and the Montreal-Cambridge-Tololo survey (Lamontagne et al. 2000).

The main goal of both the HES and the HQS survey is the compilation of a large sample of bright QSOs. In a first step QSO candidates are selected by various broadband color criteria and feature detection algorithms applied to spectra derived from low resolution scans of the prism plates (Wisotzki et al. 2000). Since among UV excess objects (i.e. $U-B<-0.4$) less than 10% can be expected to be QSOs, the Hamburg Quasar Survey and the Hamburg/ESO Survey are also a rich source of white dwarfs of various types, and early-type subdwarfs. In a recent paper, Homeier et al. (1998) present an analysis of 80 DA white dwarfs detected through follow-up observations of the HQS. Reimers et al. (1994, 1996, 1998) reported on the detection of several new magnetic white dwarfs in the HES. A summary of helium-rich subluminous stars can be found in Heber et al. (1996) and an analysis of 47 sdO stars from the HQS in Lemke et al. (1997).

In this paper we present the analysis of 40 helium-rich white dwarfs using LTE model atmospheres. The objects have been found in the HES and have entered the quasar candidate sample because of $U-B\leq -0.18$. Due to the high spectral resolution of the HES spectra (~ 15 Å at Hγ), it is possible to identify most of the hot stars in the quasar candidate sample (see Reimers & Wisotzki 1997 for example spectra) by their hydrogen and/or helium absorption lines. Featureless, *very* hot stars can be identified by their continuum shape. Therefore, the sample of stars presented in this paper is restricted to a temperature regime of $10000\,\mathrm{K}< T_{\rm eff}\leq 20000\,\mathrm{K}$ – as the analysis shows – in which neither strong absorption lines of helium nor a continuum shape notably different from that of a quasar are present. Because it was not possible to make a definitive distinction between quasars and stars on the basis of the HES objective prism spectra alone, spectroscopic follow-up observations have been performed.

2. Observational data

In Table 1 and Table 2 we summarize the follow-up spectroscopy and give coordinates, magnitudes, names from other surveys, and spectral types, if already existing, for the observed helium-rich white dwarfs. The instruments used for spectroscopy were the ESO Faint Object Spectrograph and Camera (EFOSC), the

Send offprint requests to: S. Friedrich

⋆ Based on observations collected at the European Southern Observatory, La Silla, Chile. This research has made use of the Simbad database operated at CDS, Strasbourg, France, and of the Digitized Sky Survey, produced at the Space Telescope Science Institute under US Government grant NAG W-2166.

⋆⋆ Tables 2 and 3, and Figs. 1-6 are also available at the CDS via anonymous ftp to cdsarc.u-strasbg.fr (130.79.128.5)

Table 1. Journal of observations

Date	Tel.	Instr./CCD	Grism Grat.	Resol. [Å]
Dec 1990	3.6 m	EFOSC1/RCA	B300	26
Apr 1991	3.6 m	EFOSC1/RCA	B300	26
Feb 1992	2.2 m	EFOSC2/Tek	#1	40
Feb 1992	3.6 m	EFOSC1/Tek	B300	16
Apr 1992	3.6 m	EFOSC1/Tek	B300	19
Sep 1992	3.6 m	EFOSC1/Tek	B300	21
Mar 1993	3.6 m	EFOSC1/Tek	B300	21
Mar 1993	1.52 m	B&C/LORAL	#2	15
Feb 1994	1.52 m	B&C/LORAL	#16	8
Sep 1994	3.6 m	EFOSC1/Tek	B300	21
Nov 1994	1.52 m	B&C/LORAL	#13	15
Oct 1995	1.52 m	B&C/LORAL	#13	15
Mar 1996	1.52 m	B&C/#39	#13	15
Oct 1996	1.52 m	B&C/#39	#13	15
Oct 1997	1.52 m	B&C/#39	#13	15
Sep 1998	1.52 m	B&C/#39	#13	15
Nov 1998a	1.54 m	DFOSC/LORAL	#4	10
Nov 1998b	1.54 m	DFOSC/LORAL	#11	15
Nov 1998c	1.54 m	DFOSC/LORAL	#7	5

Danish Faint Object Spectrograph and Camera (DFOSC), and the Boller & Chivens Spectrograph (B&C). A # in Table 1 refers to ESO numbering of grisms, for which details can be found in the according telescope manuals. In general a spectral range between about 3800Å and 7000Å up to 9000Å is covered with resolutions between about 100 to 500 Å/mm. The coordinates have been derived from the Digitized Sky Survey I (DSS-I). Therefore, finding charts can easily be obtained from the online DSS-I. Magnitudes are given as B_J magnitude, which is defined by the sensitivity curve of the hyper-sensitized Kodak IIIa-J emulsion combined with the filter function of a Schott BG395 filter. B_J is roughly equal to B for objects around $B-V=0$ and accurate to better than $\pm\,0\overset{\mathrm{m}}{.}2$ for all sample stars.

The spectra of all DB white dwarfs are depicted in Fig. 1 to 3. The spectra of DBA and DBAZ white dwarfs can be found in Fig. 4 and Fig. 5, respectively, and the spectra of the DZ, DQ, and DC white dwarfs are summarized in Fig. 6.

3. Spectral analysis

3.1. Models

In order to derive effective temperatures the observed spectra have been fitted to model spectra of nearly pure helium atmospheres with a small admixture of hydrogen (10^{-6} relative to helium by number) covering a temperature range from 10000 K to 35000 K in 250 K steps up to 16000 K, in 500 K steps between 16000 K and 20000 K, and 1000 K steps above 20000 K. $\log g$ was given between 7.75 and 8.5 in 0.25 dex increments. Between 16500 K and 20000 K we extended the grid to $\log g = 9$. He I line profiles were calculated with our LTE atmosphere codes (see Finley et al. 1997 for a recent description) in which the improved He I line broadening theory of Beauchamp et al. (1997) was implemented. These Stark profiles have been calculated for temperatures ranging from 10000 K to 40000 K and consider broadening by ions and electrons. Line broadening by neutral perturbers, which becomes important at lower temperatures, was not included in our calculation of line profiles. This might lead to some uncertainties. However, a temperature determination from the continuum slopes of HE 0446−2531 and HE 0449−2554, for which we have absolutely calibrated flux spectra, showed the deviation in $T_{\rm eff}$ to be less than 1000 K at temperatures of about 12000 K.

3.2. Determination of $T_{\rm eff}$

Effective temperature and $\log g$ were determined in a χ^2 fitting procedure based on a Levenberg-Marquard algorithm (cf. Press et al. 1992) by comparison of He I line profiles with synthetic spectra from the He/H atmospheres. The method is very similar to that described in detail in Homeier et al. (1998).

We started the fitting procedure with both temperature and $\log g$ as a free parameter. However, at the given data quality the dependence on $\log g$ turned out to be rather small, and it was thus not possible to determine it unambiguously. In most cases a higher $\log g$ could be compensated by a higher temperature, and vice versa, with roughly the same χ^2 value. Furthermore, systematic effects like small differences in the starting values for $T_{\rm eff}$ and $\log g$ might change the solution by much more than the statistical errors. We therefore determined $T_{\rm eff}$ for $\log g$ fixed to 8, too. Comparison of temperatures derived from fits with $\log g$ as free parameter and fixed to 8 only revealed small differences, which could often be regarded as equal within their statistical errors. This is reflected by the mean of all fitted $\log g$ values of 8.15±0.24. In Table 3 we have compiled the results of our analysis. The given errors for temperatures and $\log g$ are formal statistical errors from the covariance matrix of the fit, which do not reflect any systematic errors. As it has been discussed by many authors using similar methods (see e.g. Homeier et al. 1998; Napiwotzki et al. 1999), external errors can be higher by a large factor.

3.3. Determination of hydrogen and metal abundances

As for the DB stars, $T_{\rm eff}$ was determined for DBA and DBAZ white dwarfs by comparing He I line profiles with those from synthetic spectra of our He/H atmospheres. We did not perform selfconsistent calculations with hydrogen and metal lines already included in the atmospheres. In the next step model atmospheres for the derived effective temperatures were calculated which contain calcium and/or hydrogen in estimated amounts for the respective star. The resulting temperature and pressure stratification was then used to compute detailed synthetic spectra with varying calcium and/or hydrogen abundances. For HE 0446−2531 also magnesium and iron were considered. Abundances were then obtained by comparison of observed equivalent widths and line profiles to those from the synthetic spectra. Unless otherwise mentioned, equivalent

Table 2. Coordinates, magnitudes, cross-references and spectral types, if already existing, for the observed objects. Cross-references were taken from the Simbad database and McCook & Sion (1999). Most of the EC objects are listed in Kilkenny et al. (1997). Details of individual observing campaigns can be found in Table 1. The survey fields, given in column "field", are ESO/SERC atlas fields. The B_J magnitudes are accurate to better than $0\overset{\mathrm{m}}{.}2$.

Name	Other Names	Type	Campaign		t [s]	Field	α(2000)	δ(2000)	B_J
HE 0004−1452	PHL665		98a	Nov 1.54m	1800	607	00 06 36.0	−14 36 14	17.1
HE 0052−2511	CT195		95	Oct 1.52m	900	474	00 54 46.7	−24 55 29	17.9
HE 0104−3056	[c]		94	Sep 3.6m	300	412	01 07 12.4	−30 40 16	17.3
HE 0108−3036			92	Sep 3.6m	300	412	01 11 06.3	−30 20 34	17.7
HE 0122−2244	KUV01223-2245		97	Oct 1.52m	300	476	01 24 44.6	−22 29 07	16.8
HE 0127−3110	BPM47178, GD1363	DAH[a]	98a	Nov 1.54m	900	413	01 29 56.2	−30 55 08	16.0
			92	Sep 3.6m	300				
			98c	Nov 1.54m	1800				
HE 0149−2518	[b]		97	Oct 1.52m	600	477	01 51 59.5	−25 03 15	17.1
HE 0200−5556			96	Oct 1.52m	300	153	02 01 57.9	−55 42 16	17.5
HE 0203−5013	JL281[d]		96	Oct 1.52m	300	197	02 05 03.1	−49 59 03	17.0
HE 0308−1313	[c]		98b	Nov 1.54m	300	616	03 11 07.2	−13 01 53	17.1
HE 0309−2105	EC03097−2105		98c	Nov 1.54m	1000	547	03 11 58.1	−20 54 09	15.6
HE 0319−4344			95	Oct 1.52m	300	248	03 21 10.1	−43 34 00	17.7
HE 0413−3306			92	Feb 2.2m	300	360	04 15 20.6	−32 59 11	15.9
HE 0423−5502			95	Oct 1.52m	900	157	04 24 32.5	−54 55 38	16.9
HE 0442−3027			96	Oct 1.52m	1660	421	04 44 29.4	−30 21 36	16.2
HE 0446−2531			97	Oct 1.52m	480	485	04 49 01.4	−25 26 36	16.9
HE 0449−2554			98a	Nov 1.54m	1200	485	04 51 53.8	−25 49 15	16.5
			94	Nov 1.52m	1800				
			98a	Nov 1.54m	1200				
HE 0453−4423			95	Oct 1.52m	900	251	04 55 22.8	−44 18 19	16.8
HE 0956−1121	EC09565−1121	DB	93	Mar 3.6m	300	709	09 59 01.3	−11 35 24	16.9
HE 1002−1929			93	Mar 3.6m	300	567	10 05 02.8	−19 44 29	17.1
HE 1102−1850			93	Mar 3.6m	300	570	11 05 09.2	−19 07 05	17.1
HE 1109−1953	EC11091−1953	DB	93	Mar 3.6m	300	570	11 11 40.2	−20 09 37	16.0
HE 1128−1421	EC11285−1421	DB	96	Mar 1.52m	300	641	11 31 05.5	−14 38 09	16.7
HE 1128−1524			96	Mar 1.52m	300	641	11 30 51.7	−15 41 26	17.4
HE 1130−0111			96	Mar 1.52m	300	858	11 33 25.9	−01 28 30	17.6
HE 1145+0145			96	Mar 1.52m	300	858	11 48 33.6	+01 28 59	17.2
HE 1146−0109			96	Mar 1.52m	300	858	11 48 51.7	−01 26 12	17.3
HE 1149−1320	PG1149-133, EC11492	DB2	92	Feb 2.2m	300	642	11 51 50.5	−13 37 14	16.1
HE 1214−2017			96	Mar 1.52m	300	573	12 16 49.9	−20 33 56	17.6
HE 1243−2134	EC12436−2134		96	Mar 1.52m	300	574	12 46 18.5	−21 50 57	16.3
HE 1308−1458			91	Apr 3.6m	300	646	13 11 12.9	−15 14 28	17.2
HE 1350−1612			92	Feb 3.6m	300	649	13 53 34.9	−16 27 05	17.3
HE 1352+0026	PG1352+004	DB4	96	Mar 1.52m	300	865	13 55 32.4	+00 11 24	16.1
HE 1409−1821			93	Mar 3.6m	300	578	14 11 48.6	−18 35 04	15.6
HE 1420−1914			96	Mar 1.52m	300	579	14 23 24.1	−19 27 54	17.3
HE 1421−0856			93	Mar 3.6m	300	722	14 24 37.9	−09 09 57	17.3
HE 1428−1235	EC14289-1235		92	Apr 3.6m	300	650	14 31 39.6	−12 48 56	15.9
HE 2147−0950	[c]		98	Sep 1.52m	300	744	21 49 55.7	−09 36 31	16.6
HE 2237−0509	[c]		98	Sep 1.52m	300	819	22 39 40.7	−04 54 17	14.0
HE 2237−3630	LHS 3841, LP984-76		98	Sep 1.52m	480	406	22 40 05.2	−36 15 20	17.6

[a] classified as magnetic WD without detectable polarization in McCook & Sion (1999), Magnetic white dwarf with a polar field strength of 176 MG (Reimers et al.1996).
[b] mistakenly identified as PHL1201 in Lamontagne et al. (2000)
[c] coincidences with PHL objects (PHL3345, PHL1477, PHL166, PHL363) have been rejected using finding charts provided by E. Chavira
[d] finding chart from Jaidee & Lyngå (1969)

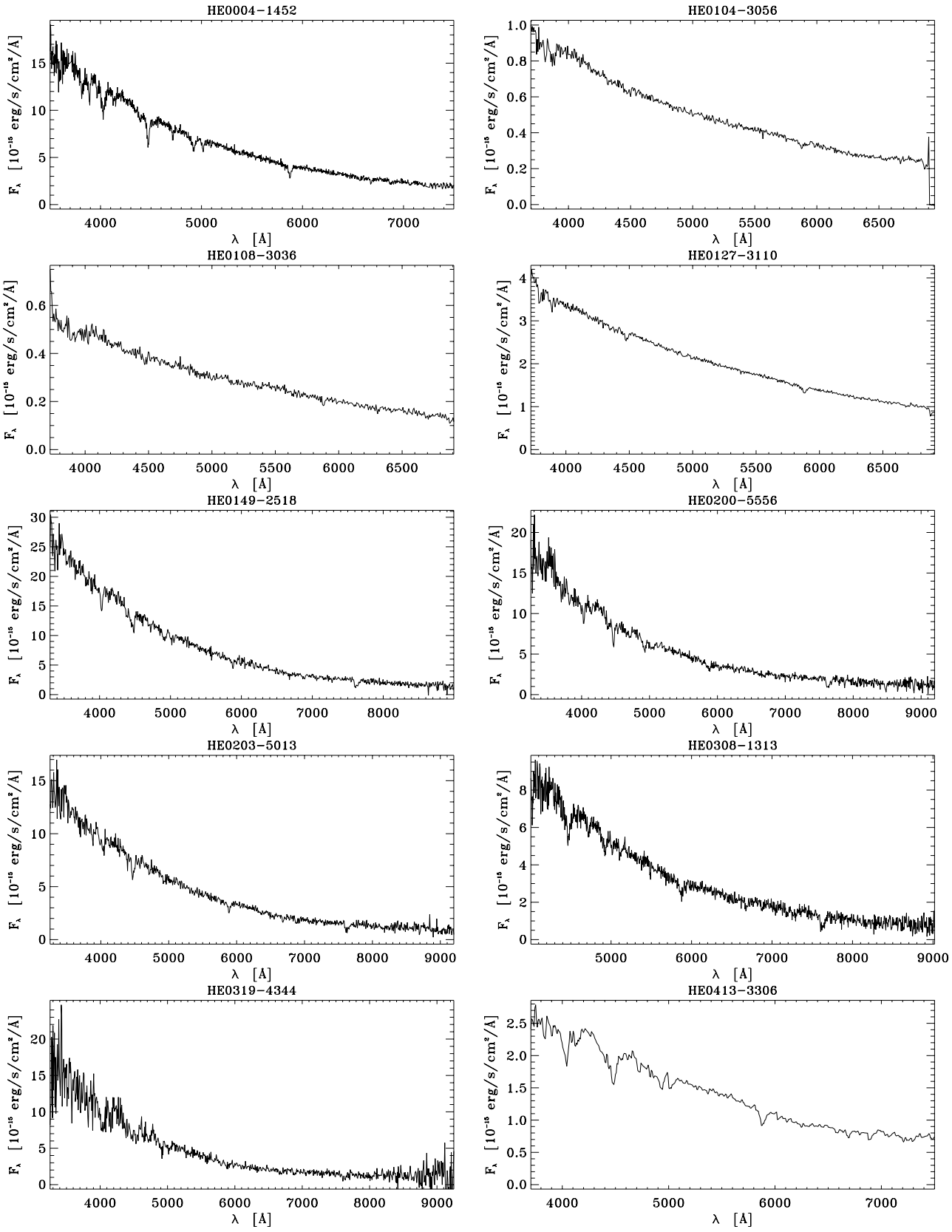

Fig. 1. DB white dwarfs

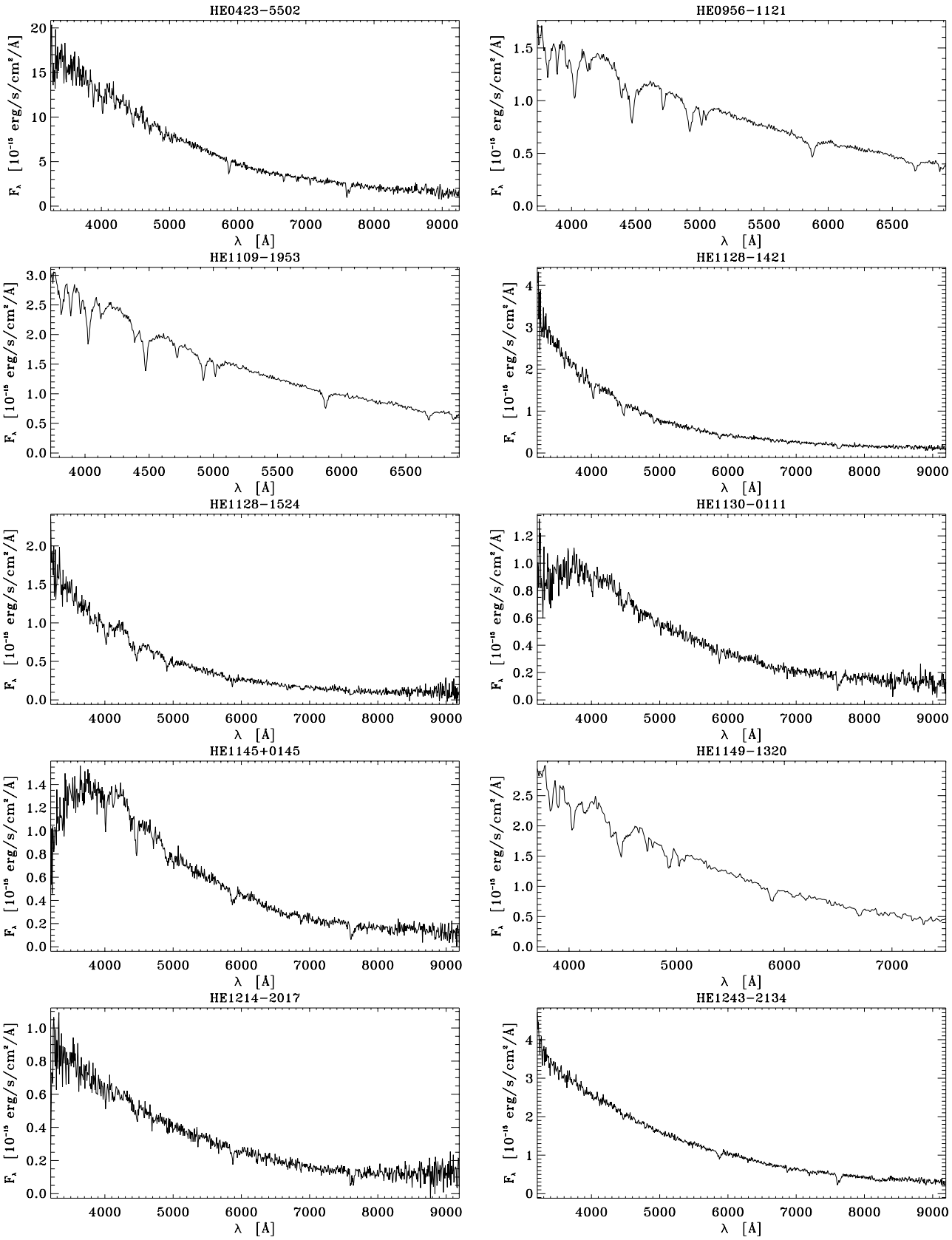

Fig. 2. DB white dwarfs (continued)

Table 3. Results from the temperature and $\log g$ determination and derived spectral types for the analyzed stars. Equivalent widths are given in Ångström

Name	Type	$T_{\rm eff}$	$\log g$	$T_{\rm eff}$ for $\log g = 8$	Remarks
HE 0004−1452	DB	16800±100	8.17±0.06	16700±100	
HE 0104−3056	DB	12600±320	8.11±0.30	12500±580	
HE 0108−3036	DB	13600±260	8.36±0.21	13200±430	
HE 0127−3110	DB	13800±120	8.48±0.09	13500±130	variable (?), possibly magnetic
HE 0149−2518	DB	16900±280	8.21±0.17	16500±310	
HE 0200−5556	DB	18500±250	8.26±0.12	17900±230	
HE 0203−5013	DB	16200±310	8.37±0.20	16000±290	
HE 0308−1313	DB	18000±170	8.90±0.20	18000±350	
HE 0319−4344	DB	18400±710	7.82±0.39	18600±800	
HE 0413−3306	DB	16600±70	7.80±0.05	16700±70	
HE 0423−5502	DB	15600±200	8.12±0.14	15500±200	
HE 0446−2531	DBAZ	12600±250	7.77±0.23	12600±280	W(λ)=50.7^{+5}_{-3}/54.3 ± 5 (Ca II, Oct97/Nov98), W(λ)=8.6 ± 1 (Hα), W(λ)=4.7 ± 0.5 (Hβ), W(λ)=$2.9^{+0.5}_{-1.0}$ (Hγ)
HE 0449−2554	DBAZ	12500±220	8.23±0.15	12200±290	W(λ)=25.0^{+2}_{-3}/22.8^{+2}_{-3} (Ca II, Nov94/Nov98) W(λ)=2.8 ± 0.5 (Hα)
HE 0956−1121	DB	18800±90	8.02±0.04	18400±80	
HE 1002−1929	DBA	16500±100	8.26±0.06	16200±100	W(λ)=3.6 ± 1 (Hα)
HE 1102−1850	DBA	17000±100	8.25±0.06	16700±120	W(λ)=2.4 ± 0.6 (Hα), W(λ)=1.1 ± 0.6 (Hβ)
HE 1109−1953	DB	17100±70	7.85±0.04	17000±60	
HE 1128−1421	DB	16900±240	8.04±0.14	16600±240	
HE 1128−1524	DB	26800±1420	8.33±0.16	27800±1120	
HE 1130−0111	DB	15000±300	8.00±0.19	15100±330	
HE 1145+0145	DB	16900±250	8.02±0.15	16600±250	
HE 1149−1320	DB	17300±120	8.07±0.07	17600±130	
HE 1214−2017	DB	16700±200	8.05±0.12	15700±210	
HE 1243−2134	DB	13800±240	8.44±0.15	13300±280	
HE 1308−1458	DB	19500±190	8.35±0.07	18800±170	
HE 1350−1612	DBAZ	15000±80	8.28±0.06	14600±90	W(λ)=8 ± 1 (Ca II), W(λ)=$2.2^{+0.3}_{-0.5}$ (Hα), W(λ)=1 ± 0.5 (Hβ)
HE 1352+0026	DB	15700±150	8.09±0.10	15400±170	
HE 1409−1821	DB	18400±110	7.88±0.06	18300±130	
HE 1420−1914	DB	17900±220	8.24±0.12	17200±370	
HE 1421−0856	DB	17100±90	7.84±0.05	17200±90	
HE 1428−1235	DB	19500±50	7.87±0.02	19500±60	
HE 2147−0950	DBA	14600±220	8.17±0.13	14100±410	W(λ)=3.5 ± 0.5 (Hα)
HE 2237−0509	DBA	13300±360	8.34±0.27	12900±380	W(λ)=3.4 ± 1 (Hα)
Possible helium-rich stars without helium lines					
HE 0052−2511		—	—	—	possibly DC or magnetic
HE 0122−2244	DZ	—	—	10000^{+2000}_{-1000}	W(λ)=18.4^{+3}_{-5}/19.0 ± 2 (Ca II, Oct97/Nov98)
HE 0309−2105	DC	—	—	—	
HE 0442−3027		—	—	—	possibly DC or DQ
HE 0453−4423	DC	—	—	—	
HE 1146−0109	DQ	—	—	—	C_2 bands
HE 2237−3630	DC	—	—	—	binary

widths of Hα, Hβ, and Hγ were determined between 6543 Å and 6583 Å, 4841 Å and 4881 Å, and 4310 Å and 4370 Å, respectively; equivalent widths of the Ca II doublet were determined between 3890 Å and 3990 Å.

When comparing HE 0446-2531 and HE 0449-2554, the great difference in calcium abundances (approximately a factor of 30) is surprising because temperatures are similar, and equivalent widths differ only by a factor of 2. However, their hydrogen abundances also differ by about a factor of 20. This affects the atmospheric structure since hydrogen contributes electrons, and changes the opacity. In turn the changed atmospheric structure does influence the line spectrum.

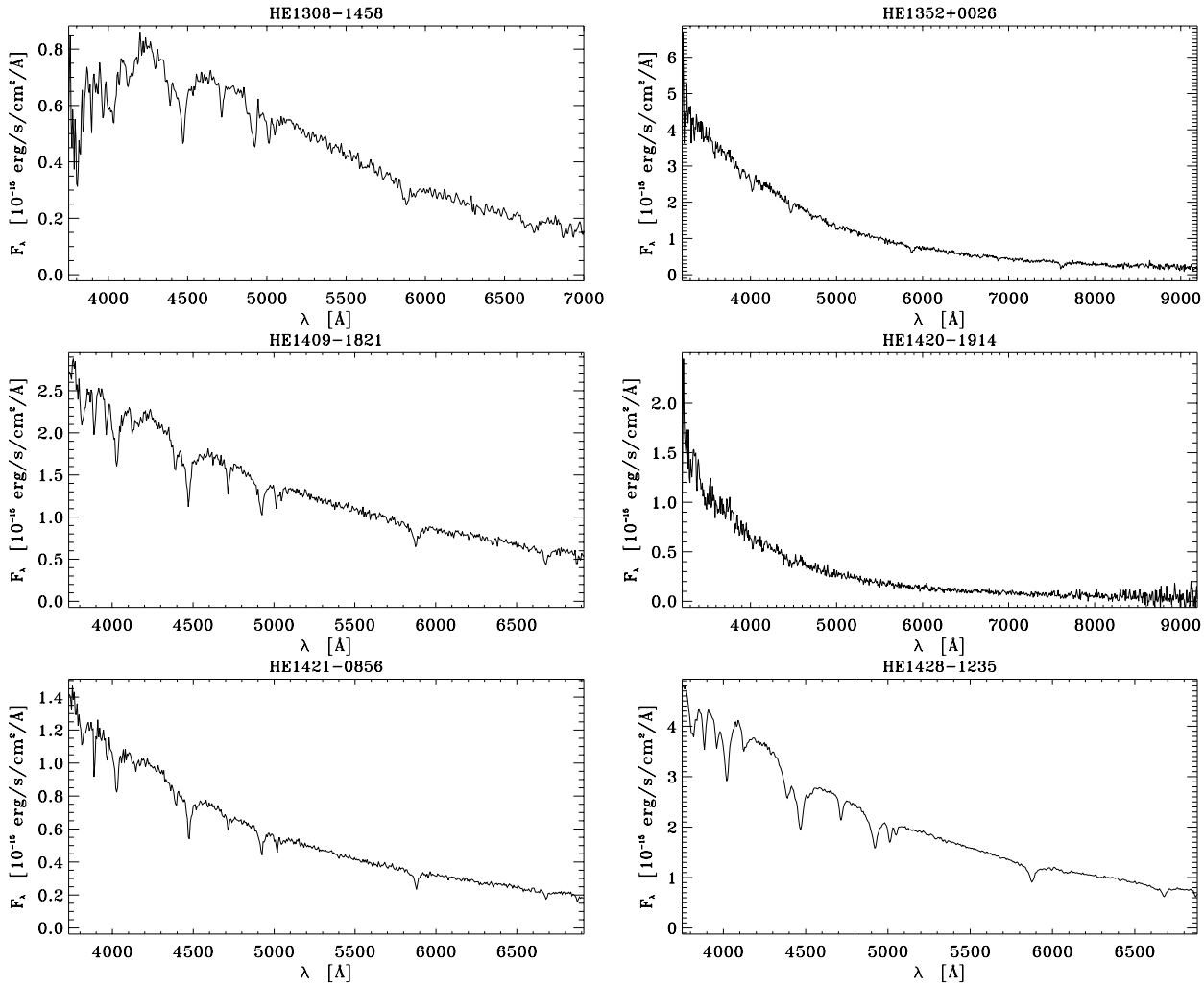

Fig. 3. DB white dwarfs (continued)

4. Discussion of individual objects

4.1. DB white dwarfs

4.1.1. HE 0127−3110

HE 0127−3110 was observed several times during the follow-up observations performed for the HES: Spectra were obtained in September 1992 (used here), September 1994, November 1994, and November 1998. Spectra from 1994 show broad absorption troughs, varying in depth and profile, whereas the September 1992 spectrum resembles a DB spectrum. After a careful inspection of individual telescope pointings to exclude the accidental observation of a different star, we conclude that HE 0127−3110 is variable.

The only common feature of all spectra is an absorption line at 5876 Å which can be attributed to He I. The broad absorption features in the spectra of 1994 led to the classification as a magnetic DA white dwarf with a polar field strength of 176 MG (Reimers et al. 1996). In this scenario the putative He I line at 5876 Å is due to a hydrogen Hα component ($2s_0 \rightarrow 3p_0$), which becomes stationary only at a field strength of 235 MG with a minimum wavelength of 5830 Å. It is interesting to mention that HE 2201−2250, whose spectrum looked almost identical to the 1994 spectra of HE 0127−3110 (Reimers et al. 1996), meanwhile also changed its spectroscopic appearance to a DB white dwarf. A detailed discussion will be published in a forthcoming paper.

4.2. DBA white dwarfs

4.2.1. HE 1002−1929 and HE 1102−1850

In the spectra of HE 1002−1929 and HE 1102−1850 the Hα line is clearly visible with equivalent widths of (3.6 ± 1) Å and (2.4 ± 0.6) Å, respectively. The Hβ line (W(λ)=(1.1 ± 0.6) Å) can be detected only in the spectrum of HE 1102−1850, despite the larger equivalent width of Hα in HE 1002−1929 and a similar temperature. From the equivalent widths we calculated hydrogen abundances of $(5^{+5}_{-2}) \cdot 10^{-5}$ and $(2^{+2}_{-1}) \cdot 10^{-5}$ for HE 1002−1929 and HE 1102−1850, respectively. Metal lines could not be detected.

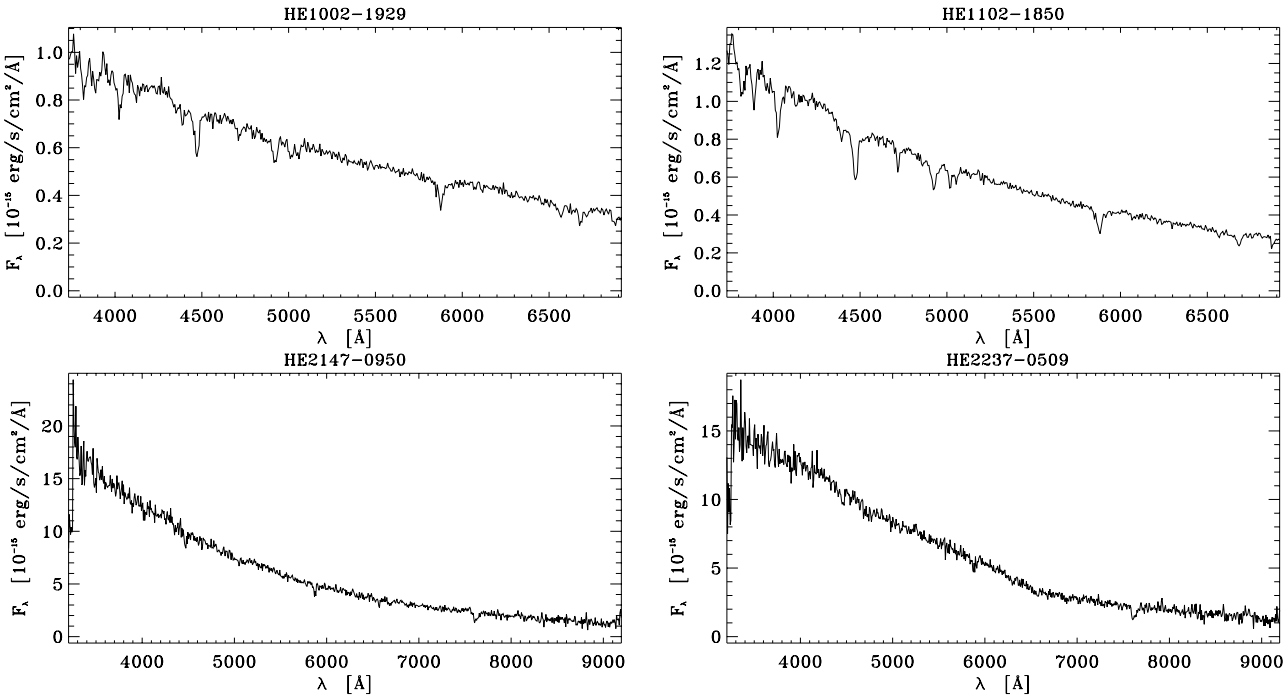

Fig. 4. DBA white dwarfs

4.2.2. HE 2147−0950 and HE 2237−0509

HE 2147−0950 and HE 2237−0509 show absorption features at the position of Hα with equivalent widths of (3.5 ± 0.5) Å and (3.4 ± 1.0) Å, respectively. Because both spectra are very noisy, this should be taken with caution. The measured equivalent widths would correspond to hydrogen abundances of $(4 \pm 2) \cdot 10^{-5}$ and $(6 \pm 4) \cdot 10^{-5}$, respectively.

4.3. DBAZ white dwarfs

4.3.1. HE 0446−2531

The most prominent lines in the November 1998 spectrum of HE 0446−2531 are hydrogen lines of the Balmer series up to Hγ, the He I line at 4471 Å and a somewhat weaker He I line at 5876 Å. The October 1997 spectrum is too noisy to let the Balmer lines be discerned. Equivalent widths for Hα and Hβ were determined between 6530 Å and 6590 Å, and 4820 Å and 4885 Å, respectively. Together with the equivalent width of Hγ they result in a hydrogen abundance of $(7^{+3}_{-2}) \cdot 10^{-4}$. The equivalent width of the calcium doublet was determined between 3850 Å and 4050 Å to comprise the whole doublet. This is justified because the He I line at 4026 Å is to weak to significantly contribute. The calcium abundance derived from an equivalent width of (52.5^{+5}_{-6}) Å (unweighted mean from the October 97 and November 98 spectrum) amounts to $(2 \pm 1) \cdot 10^{-6}$. At 3704 Å, 3735 Å, 3834 Å, and 5170 Å lines can be detected, which are most probably due to neutral magnesium and neutral as well as ionized iron. With this assumption we derive abundances of $(2^{+3}_{-1}) \cdot 10^{-6}$ and $(2 \pm 1) \cdot 10^{-6}$ for magnesium and iron, respectively.

Table 4. Element abundances (relative to helium) for the DBA, DBAZ, and DZ white dwarfs

object	Type	H	Mg	Ca	Fe
		10^{-5}	10^{-6}	10^{-8}	10^{-6}
HE 0122−2244	DZ			$0.04^{+0.01}_{-0.02}$	
HE 0446−2531	DBAZ	70^{+30}_{-20}	2^{+3}_{-1}	200 ± 100	2 ± 1
HE 0449−2554	DBAZ	3 ± 1		7 ± 2	
HE 1002−1929	DBA	5^{+5}_{-2}			
HE 1102−1850	DBA	2^{+2}_{-1}			
HE 1350−1612	DBAZ	2 ± 1		20^{+10}_{-15}	
HE 2147−0950	DBA	4 ± 2			
HE 2237−0509	DBA	6 ± 4			

4.3.2. HE 0449−2554

Since the November 94 spectrum is very noisy HE 0449-2554 was reobserved in November 1998. Besides the doublet of calcium at 3934 Å and 3968 Å already seen in the November 94 spectrum, the new spectrum clearly shows an Hα line. At 4471 Å and 5876 Å also weak features can be spotted. They are consistent with line depths and line strengths of corresponding He I lines in a synthetic spectrum with $T_{\rm eff}$ = 12200 K. The equivalent width of the Hα line ((2.8 ± 0.5) Å) corresponds to a hydrogen abundance of $(3 \pm 1) \cdot 10^{-5}$. The unweighted mean equivalent width of the calcium doublet from both observing runs (23.9^{+2}_{-3} Å) was taken to determine a calcium abundance of $(7 \pm 2) \cdot 10^{-8}$.

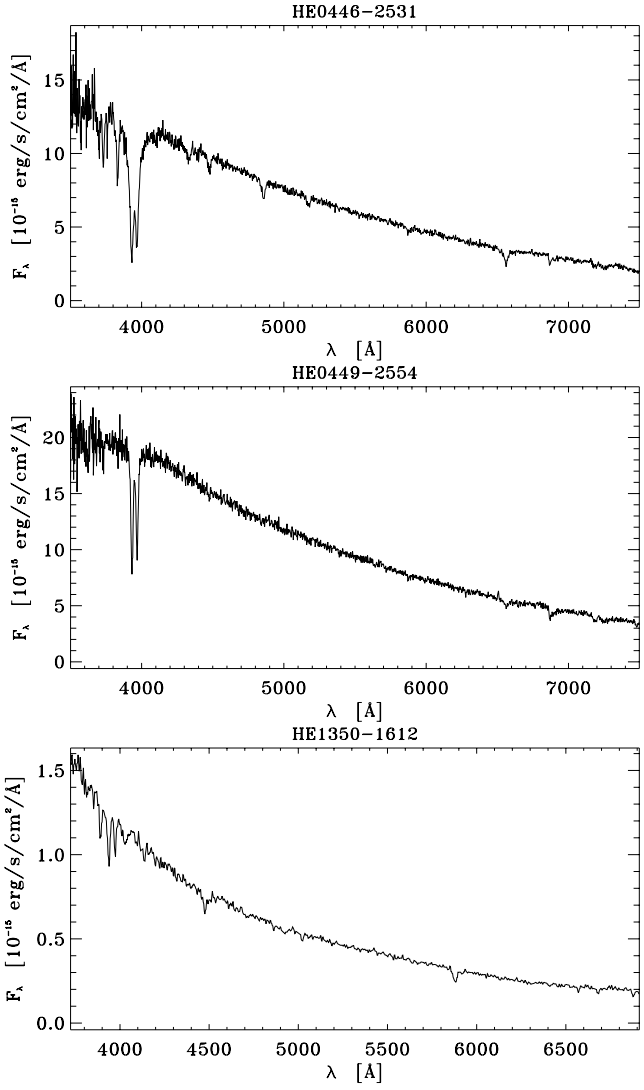

Fig. 5. DBAZ white dwarfs

4.3.3. HE 1350−1612

In addition to He I lines also Hα, Hβ, and the Ca II doublet at 3934 Å and 3968 Å can be detected in the spectrum. With an effective temperature of 14600±90 K, this star is one of the very few DBAZ stars in the temperature range of about 15000 K, where He I lines make temperature determinations reliable. The only other such star known is HS 2253+8023 (Friedrich et al. 1999a, 1999b), and perhaps GD40, with a published equivalent width of Hα of 1 Å (Greenstein & Liebert 1990). Hydrogen and calcium abundances determined from equivalent widths amount to $(2 \pm 1) \cdot 10^{-5}$ and $(2^{+1.0}_{-1.5}) \cdot 10^{-7}$, respectively.

4.4. DZ white dwarfs

4.4.1. HE 0122−2244

The Ca II doublet at 3934 Å/3968 Å and an otherwise featureless spectrum classify HE 0122−2244 as a DZ white dwarf. An approximate temperature of 10000^{+2000}_{-1000} K for $\log g = 8$ was determined from the continuum slope of the photometric November 98 spectrum. For this temperature the equivalent width of the Ca II doublet (18.7^{+4}_{-5} Å, unweighted mean) corresponds to a calcium abundance of $(4^{+1}_{-2}) \cdot 10^{-10}$.

4.5. DC and DQ white dwarfs

4.5.1. HE 0052−2511

Weak flux depressions at 5000 Å and 6300 Å are the only features in the observed spectral range from 3500 Å to 9200 Å. Therefore, this star might be of type DC, or possibly a magnetic white dwarf. If this star is magnetic, the main constituent of its atmosphere could be helium, because helium, contrary to hydrogen, has no stationary components and hence has no detectable features over a wide range of field strengths (Schmelcher, priv.comm.).

4.5.2. HE 0309−2105

HE 0309−2105 was already observed by Sefako et al. (1999). On the basis of its colours ($B - V = 0.10 \pm 0.05$, $U - B = -0.08 \pm 0.05$) derived from UBV photometry they were not able to classify the object. However, our synthetic colours derived from prism plates of the HES and confirmed by spectroscopy yield $B - V = -0.10 \pm 0.08$ and $U - B = -0.88 \pm 0.08$, respectively, which place HE 0309−2105 well in the regime of white dwarfs in the two-colour diagram. Together with its featureless spectrum it is therefore classified as DC.

4.5.3. HE 0442−3027

C_2 bands might be the reason for weak flux depressions at 4700 Å and 5100 Å. Therefore, HE 0442−302 might rather be a DQ than a DC.

4.5.4. HE 1146−0109

HE 1146−0109 displays strong C_2 bands at 4670 Å and 5140 Å. Since no other features can be detected in the spectrum, the star is classified as DQ.

4.5.5. HE 2237−3630

This star has a composite spectrum, which shows no clear features bluewards of 5800 Å, and strong TiO bands redwards of 5800 Å. There are hints for absorption features at 3730 Å and 4026 Å, which could be attributed to helium, and one at 5170 Å, which could possibly be due to magnesium and iron. We assume that HE 2237−3630 is a binary star with a helium-rich white dwarf component and a M-dwarf component.

5. Discussion

We have presented a model atmosphere analysis of cool helium-rich white dwarfs found in the Hamburg/ESO survey for which follow-up spectroscopy has been performed. Since the selec-

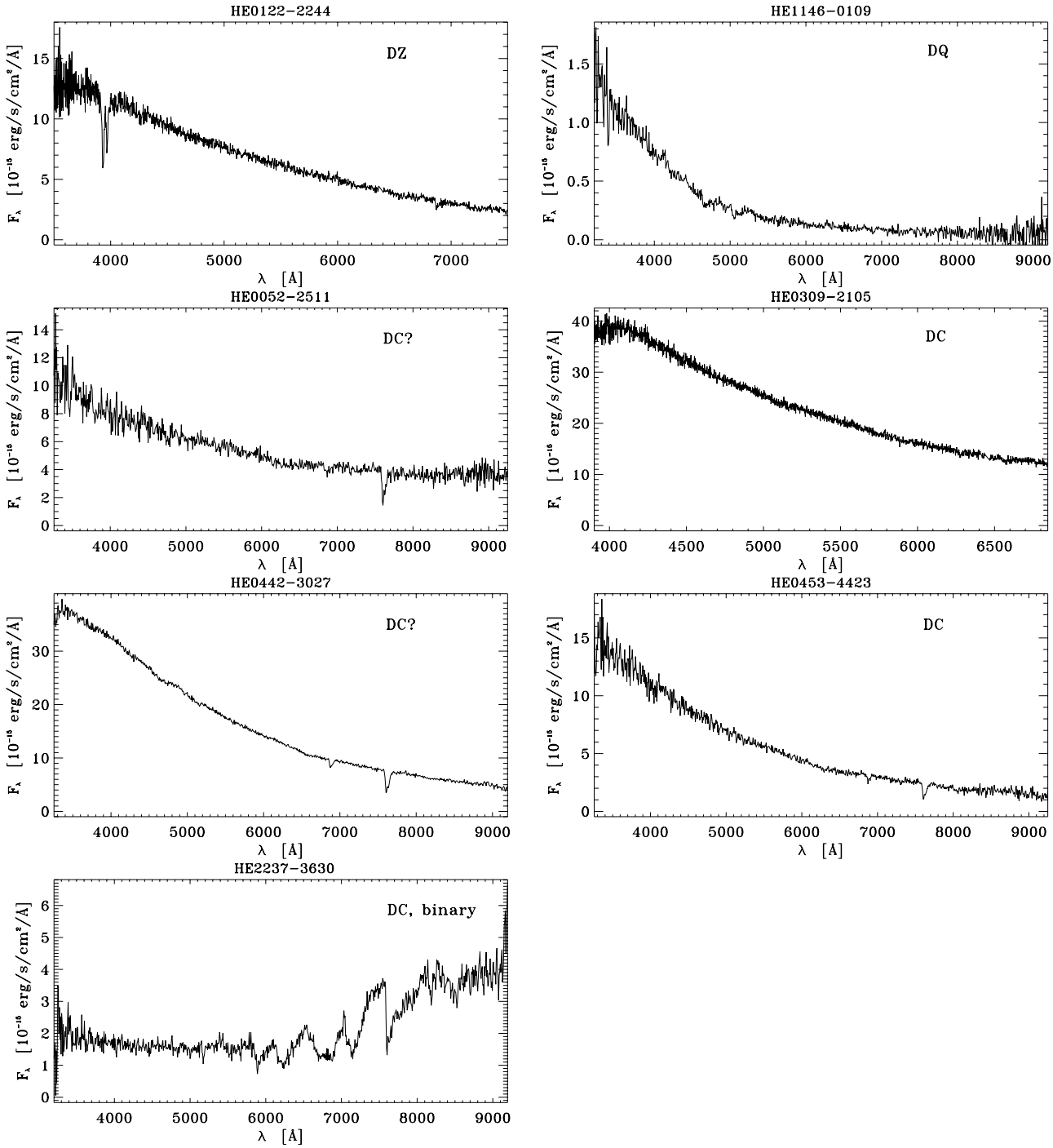

Fig. 6. DZ, DQ, and DC white dwarfs

tion criterium for these stars was confined to a continuum slope similar to QSOs, and no strong absorption lines, this sample of helium-rich white dwarfs is biased towards $T_{\rm eff}$ below 20000 K.

Among the 33 analyzed DB stars, we found 4 DBA, if we include HE 2147−0950 and HE 2237−0509 with a somewhat uncertain identification of Hα, and 3 DBAZ stars; hence, a fraction of 21% in our sample shows traces of hydrogen. This is consistent with the findings of Shipman et al. (1987), who found 19% DBA white dwarfs in their complete sample of cool DB stars from the Palomar-Green survey.

Especially the DBAZ stars are important in the context of the ongoing discussion of accretion of hydrogen and metals from the interstellar medium. Since the diffusion times of metals in helium-rich atmospheres are short compared to evolutionary time scales (Paquette et al. 1986), it is generally accepted that metals cannot be of primordial origin but must be accreted from the interstellar medium. Compared to the accretion-diffusion

model of Dupuis et al. (1992, 1993a, 1993b), which predicts element abundances in cool white dwarf atmospheres in consideration of accretion from the interstellar medium, the derived Ca abundances for the DBAZ stars found and the magnesium and iron abundance for HE 0446−2531 are consistent with accretion in solar element proportions at high accretion rates. For HE 0446−2531 it is also possible to determine metal-to-metal ratios. Whereas the Fe/Mg ratio falls within the predicted range, the Fe/Ca and Mg/Ca ratios are below their respective lower limits, but given the large errors they might still be compatible with accretion in solar element proportions.

Contrary to the metals, which sink down in the atmospheres and disappear very rapidly, hydrogen has the tendency to float on top of a helium-rich atmosphere. It is therefore accumulated with time in the surface layers. Thus one would expect a metal-to-hydrogen ratio, which is below the solar value. As already observed in other helium-rich metal-line white dwarfs (see Dupuis et al. 1993b for a compilation) the Ca/H ratio is larger by a factor of 10^3 to 10^4 than the solar value for the new DBAZ stars, supporting the hypothesis that accretion of hydrogen is somehow reduced compared to accretion of metals. The mechanism most widely discussed for this "hydrogen screening" is the propeller mechanism of Illarionov & Sunyaev (1975), originally developed for accretion of interstellar matter onto neutron stars. Wesemael & Truran (1982) first discussed it in the context of white dwarfs. They proposed that metals are accreted in the form of grains onto a slowly rotating, weakly magnetized (10^5 G) white dwarf, whereas ionized hydrogen is repelled at the Alfvén radius. However, it remains to be demonstrated that the necessary conditions for rotation, magnetic field and hydrogen-ionizing radiation are fulfilled to make the propeller mechanism operate.

Acknowledgements. The Hamburg/ESO Survey has been supported by the DFG under grants Re 353/33 and Re 353/40. Work on the Hamburg Quasar Survey in Kiel is supported by a grant from the DFG under Ko 738/10-3. We want to thank Dr. E. Chavira (INAOE) for supplying finding charts of PHL objects. D.K. is grateful to Dr. Jay Holberg (Lunar and Planetary Laboratory) and Dr. Jim Liebert (Steward Observatory) for their hospitality during his sabbatical at the University of Arizona.

References

Beauchamp A., Wesemael F., Bergeron P., 1997, ApJS 108, 559
Cristiani S., La Franca F., Andreani P., et al., 1995, A&AS 112, 347
Dupuis J., Fontaine G., Pelletier C., Wesemael F., 1992, ApJS 82, 505
Dupuis J., Fontaine G., Pelletier C., Wesemael F., 1993a, ApJS 84, 73
Dupuis J., Fontaine G., Wesemael F., 1993b, ApJS 87, 345
Finley D.S., Koester D., Basri G., 1997, ApJ 488, 375
Friedrich S., Koester D., Heber U., Reimers D., 1999a, In: Solheim J.-E., Meištas E. (eds.) Proceedings of the 11th European wokshop on white dwarfs. ASP Conf. Ser. vol. 169, p. 505
Friedrich S., Koester D., Heber U., Jeffery C.S., Reimers D., 1999b, A&A 350, 865
Greenstein J.L., Liebert J.W., 1990, ApJ 360, 662
Hagen H.-J., Groote D., Engels D., Reimers D., 1995, A&AS 111, 195
Heber U., Dreizler S., Hagen H.-J., 1996, A&A 311, L17
Homeier D., Koester D., Hagen H.-J., et al., 1998, A&A 338, 563
Illarionov A.F., Sunyaev R.A., 1975, A&A 39, 185
Kilkenny D., O'Donoghue D., Koen C., Stobie R.S., Chen A., 1997, MNRAS 287, 867
Jaidee S., Lyngå G., 1969, Arkiv f. Astronomi 5, 345
Lamontagne R., Demers S., Wesemael F., Fontaine G., Irwin M.J., 2000, ApJ 119, 241
Lemke M., Heber U., Dreizler S., Napiwotzki R., Engels D., 1997, In: Philip A.G.D., Liebert J., Saffer R.A. (eds.) The third conference on Faint Blue Stars. L. Davis Press, Schenectady, N.Y., p. 375
McCook G.P., Sion E.M., 1999, ApJS 121, 1
Napiwotzki R., Green P.J., Saffer R.A., 1999, ApJ 517, 399
Paquette C., Pelletier C., Fontaine G., Michaud G., 1986, ApJS 61, 197
Press W.H., Teukolsky S.A., Vetterling W.T., Flannery B.P., 1992, Numerical Recipes in FORTRAN. 2nd Edition, Cambridge University Press, Cambridge
Reimers D., Jordan S., Köhler T., Wisotzki L., 1994, A&A 285, 995
Reimers D., Jordan S., Koester D., et al., 1996, A&A 311, 572
Reimers D., Jordan S., Beckmann V., Christlieb N., Wisotzki L., 1998, A&A 337, L13
Reimers D., Wisotzki L., 1997, The Messenger 88, 14
Sefako R.R., Glass I.S., Kilkenny D., et al., 1999, MNRAS 309, 1043
Shipman H.L., Liebert J., Green R.F., 1987, ApJ 315, 239
Stobie R.S., Kilkenny D., O'Donoghue D., et al., 1997, MNRAS 287, 848
Wesemael F., Truran J.W., 1982, ApJ 260, 807
Wisotzki L., Köhler T., Groote D., Reimers D., 1996, A&AS 115, 227
Wisotzki L., Christlieb N., Bade N., et al., 2000, A&A 358, 77